# 100 % reflectivity from a monolithic dielectric micro-structured surface

Frank Brückner[a], Tina Clausnitzer[a], Oliver Burmeister[b], Daniel Friedrich[b], Ernst-Bernhard Kley[a], Karsten Danzmann[b], Andreas Tünnermann[a], and Roman Schnabel[b]

[a]Institut für Angewandte Physik, Friedrich-Schiller-Universität Jena, Max-Wien-Platz 1, 07743 Jena, Germany;
[b]Max-Planck-Institut für Gravitationsphysik (Albert-Einstein-Institut) and Institut für Gravitationsphysik, Leibniz Universität Hannover, Callinstrasse 38, 30167 Hannover, Germany

## ABSTRACT

Here, we propose a new mirror architecture which is solely based upon a monolithic dielectric micro-structured surface. Hence, the mirror device, which consists of a possibly mono-crystalline bulk material, can in principle simultaneously provide perfect reflectivity and lowest mechanical loss. By specifically structuring the monolithic surface, resulting in T-shaped ridges of a subwavelength grating, a resonant behavior of light coupling can be realized, leading to theoretically 100 % reflectivity.

**Keywords:** Resonant grating, Waveguide grating, Monolithic mirror, Micro-optical device

## 1. INTRODUCTION

In many fields of physics increased research activity is currently taking place on opto-mechanical systems in which a light field is coupled via radiation pressure to the dynamics of a mechanical oscillator or a free test mass.[1–8] The surface of the mechanical device provides the interface between the light field and the solid state matter. In many ongoing and future experiments such as laser-cooling of mechanical oscillators,[1,2] optical traps for mirrors,[3] generation of entangled test masses,[4,5] quantum non-demolition interferometry[6,7] and gravitational wave detection[7,8] this interface needs to provide outstanding low optical and mechanical losses. High reflectivity is demanded as lost photons result in decoherence of the light-matter quantum state. High mechanical quality factors are required to reduce the influence of thermal noise[9] and to reach the quantum mechanical ground state.[10] In current approaches the surface of the mechanical device is composed of a multilayer dielectric coating. Reflectivities of up to 99.9998 % have been demonstrated.[11] In order to achieve high mechanical quality factors, crystalline materials like quartz or silicon are used. Quality factors above $10^9$ were measured.[12] However, recent theoretical and experimental research revealed that multilayer dielectric coatings result in a significant reduction of quality factors[9,13] and that the simultaneous realization of high optical and mechanical quality is a non-trivial problem.

In this report we propose a highly-reflective monolithic dielectric surface, which provides a solution for the great demands mentioned above. By etching T-shaped ridges into the surface of a monolithic device, perfect reflectivity of the surface can be achieved without adding any other material.

## 2. RESONANT WAVEGUIDE GRATINGS

Advanced surface architectures have been suggested before in order to reduce the optical and mechanical loss.[14] They build on resonant waveguide gratings that comprise a periodically micro-structured high-index layer attached to a low-index substrate.[15–17] High reflectivity can be achieved by utilizing the resonant behavior of light coupling of these corrugated waveguides. Though this approach reduces the thick dielectric layer stack of

Further author information: (Send correspondence to F.B.)
F.B.: E-mail: frank.brueckner@uni-jena.de, Telephone: +49 (0) 3641 947 835, Telefax: +49 (0) 3641 947 802, www.iap.uni-jena.de

Advanced Fabrication Technologies for Micro/Nano Optics and Photonics, edited by Thomas J. Suleski, Winston V. Schoenfeld, Jian Jim Wang, Proc. of SPIE Vol. 6883, 68830X, (2008) · 0277-786X/08/$18 · doi: 10.1117/12.767775

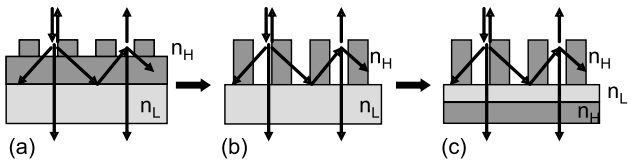


Figure 1. Different types of resonant waveguide gratings: (a) a waveguide corrugated at its surface, (b) stand-alone high-index grating ridges and (c) reduction of the low-index substrate to a layer.

conventional mirrors to a thin waveguide layer, at least one residual coating step is involved for the fabrication of such elements, thus, causing a reduction of the mechanical quality.

The fundamental principle of waveguide gratings is illustrated in Fig. 1(a). In case of normal incidence the three following parameter inequalities have to be fulfilled in order to allow for resonant reflection:

$$p < \lambda \quad \text{(to permit only 0th order in air)}, \tag{1}$$

$$\lambda/n_{\mathrm{H}} < p \quad \text{(1st orders in high-index layer)}, \tag{2}$$

$$p < \lambda/n_{\mathrm{L}} \quad \text{(only 0th order in substrate)}, \tag{3}$$

where $p$ is the grating period, $\lambda$ is the light's vacuum wavelength and $n_{\mathrm{H}}$ and $n_{\mathrm{L}}$ are the higher and lower refractive indices, respectively. In this setup, higher diffraction orders experience total internal reflection (at the boundary layer to the low-index substrate) and excite resonant waveguide modes that lead to the desired suppression of transmitted light. If $p$, the groove depth $d$, the grating duty cycle $f$ (ratio between grating ridge $b$ and period $p$) and the high-index layer thickness with respect to the refractive index values of the involved materials are designed properly, all transmitted light can be prompted to interfere destructively.[17] The fundamental diffraction order, therefore, does not transmit any power to the substrate. It has been shown previously that this is even possible with zero waveguide layer thickness, see Fig. 1(b).[16] Moreover, the low-index substrate can be reduced to a layer of some certain minimum thickness, since it just has to prevent evanescent transmission of the higher orders to the underlying substrate, see Fig. 1(c).[18] Its thickness, therefore, has to exceed a certain value, making this configuration equivalent to Fig. 1(b).

A monolithic implementation of the latter element was proposed by Ye *et al.* by replacing the low-index layer with air ($n_{\mathrm{L}} = 1$), resulting in grating ridges levitated above the substrate.[19] Though this approach allows for high reflectivity theoretically, it appears hardly capable for final applications due to a very sophisticated fabrication technique and mainly a very weak mechanical stability. Hence, it is limited to very small grating areas and highly susceptible to damage.

## 3. NEW MONOLITHIC APPROACH

For our new approach, the low-index layer in Fig. 1(c) is replaced by a low duty cycle grating, which acts as an effective medium with the effective index $n_{\mathrm{eff}} < n_{\mathrm{H}}$. This approach which aims for a resonant monolithic mirror device has, to the best of our knowledge, not been proposed before. The basic idea is illustrated in Fig. 2, revealing that the low duty cycle (LDC) grating exhibits the same period as the high duty cycle (HDC) grating on top. Since the latter generates higher diffraction orders, referring to Ineq. (2), the description of the LDC grating as an effective medium is not obvious.[20] However, this problem is solved by a sufficiently low grating duty cycle, which makes it act very similarly to a layer of air, wherein no higher diffraction orders are allowed to propagate [Ineq. (3)].

### 3.1 Phenomenological Explanation

In terms of an intelligible explanation, all involved diffraction orders have to be understood as corresponding discrete grating modes, which are excited by the incident plane wave. This consideration becomes essential if the groove depth and the grating period are of comparable dimensions.[21] In order to ensure the desired resonant

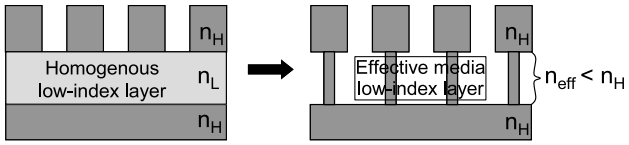


Figure 2. Proposed architecture of a monolithic low-loss surface. The low-index layer is realized by a grating with a low duty cycle, providing an effective medium ($n_{\text{eff}}$).

coupling behavior of the mirror device, two major criteria have to be fulfilled. While higher grating modes (equivalent to higher diffraction orders) need to propagate besides the fundamental 0th mode (equivalent to the 0th order) within the upper grating, no higher modes besides the 0th mode may propagate within the lower grating. A HDC grating is able to guide higher modes since it acts similarly to a homogeneous layer of the high-index material and, thus, allows for the propagation of higher orders, referring to Ineq. (2). Accordingly, a LDC grating acts similarly to a homogeneous layer of air and, referring to Ineq. (3), suppresses the propagation of higher orders or modes, respectively. Hence, a resonant excitation of higher modes within the HDC grating can be achieved, since these modes experience total internal reflection at the boundary layer to the LDC grating. In agreement with conventional waveguide gratings the fundamental mode of the small duty cycle grating does not transmit any power to the substrate due to destructive interference effects. In conclusion, the rationale of the new element corresponds quite obviously to that of conventional corrugarted waveguides as diffraction orders and grating modes can be treated similarly.

This model can be completely justified by a detailed analysis of the electric field distribution inside both gratings, according to Ref. 22, which will be the subject of a forthcoming publication.

The arising monolithic T-shaped structure which consists of a HDC grating on top of a LDC grating, as depicted in Fig. 2, can be optimized to create 100 % reflectivity for particular conditions of light incident from air, which are defined by the angle of incidence, the wavelength and the polarization state. In this approach, no material is added to the mirror device that potentially increases the mechanical loss. Very recently is was experimentally shown that a grating, etched into the surface of a substrate, did not reduce the substrate's quality factor, which was of the order $10^8$.[23]

## 3.2 Particular Design Considerations

As an example, we consider a crystalline silicon surface and calculate the parameters of a monolithic surface having nearly 100 % reflectivity for light at a vacuum wavelength of 1550 nm for normal incidence, assuming a refractive index of $n_{\text{H}} = 3.5$. In case of a very low duty cycle of the LDC grating, the effective index approaches $n_{\text{eff}} \to 1$. According to Ineqs. (2) and (3), we find an appropriate range of the grating period from $443\,\text{nm} < p < 1550\,\text{nm}$.

### 3.2.1 TM-Polarization

In case of TM-polarized light, we chose a grating period of $p = 700\,\text{nm}$. By means of rigorous simulations[24] the four parameters of both grating regions (duty cycle $f_{\text{up}}$ and $f_{\text{low}}$, groove depth $d_{\text{up}}$ and $d_{\text{low}}$) can be derived. For fixed start parameters of the lower grating ($f_{\text{low}} = 0.25$, $d_{\text{low}} = 2\ \mu\text{m}$), the upper one was optimized by simultaneously varying $f_{\text{up}}$ and $d_{\text{up}}$ in the ranges from $0.4 < f_{\text{up}} < 0.9$ and $0 < d_{\text{up}} < 800\,\text{nm}$, respectively. The resulting reflectivity is plotted in Fig. 3(a), revealing regions with a nearly perfect reflectivity (99.99 % up to 100 %) indicated by the solid line.

A highly beneficial design point is $(f_{\text{up}};d_{\text{up}}) = (0.56;350\,\text{nm})$ where high reflectivity as well as convenient fabrication tolerances are found. In order to examine the fabrication tolerances of the lower grating for the found design point, its parameters were varied as well ranging from $0 < f_{\text{low}} < 0.5$ and $0 < d_{\text{low}} < 2\ \mu\text{m}$, respectively. The plotted reflectivity in Fig. 3(b) displays a wide range of high reflectivity and supports the theoretical considerations of the preceding paragraph. For a duty cycle smaller then about 0.3, a minimal groove depth can be found which prevents transmission of higher diffraction orders to the substrate. The most beneficial parameter values arising from the simulation for TM-polarized light are, at a glance:

$$\begin{array}{rcl} n_{\mathrm{H}} & = & 3.5 \\ \lambda & = & 1550\,\mathrm{nm} \\ \phi & = & 0^\circ \\ p & = & 700\,\mathrm{nm} \end{array} \quad \Longrightarrow \quad \begin{array}{rcl} f_{\mathrm{low}} & = & 0.26 \\ d_{\mathrm{low}} & = & 430\,\mathrm{nm} \\ f_{\mathrm{up}} & = & 0.56 \\ d_{\mathrm{up}} & = & 350\,\mathrm{nm}. \end{array} \tag{4}$$

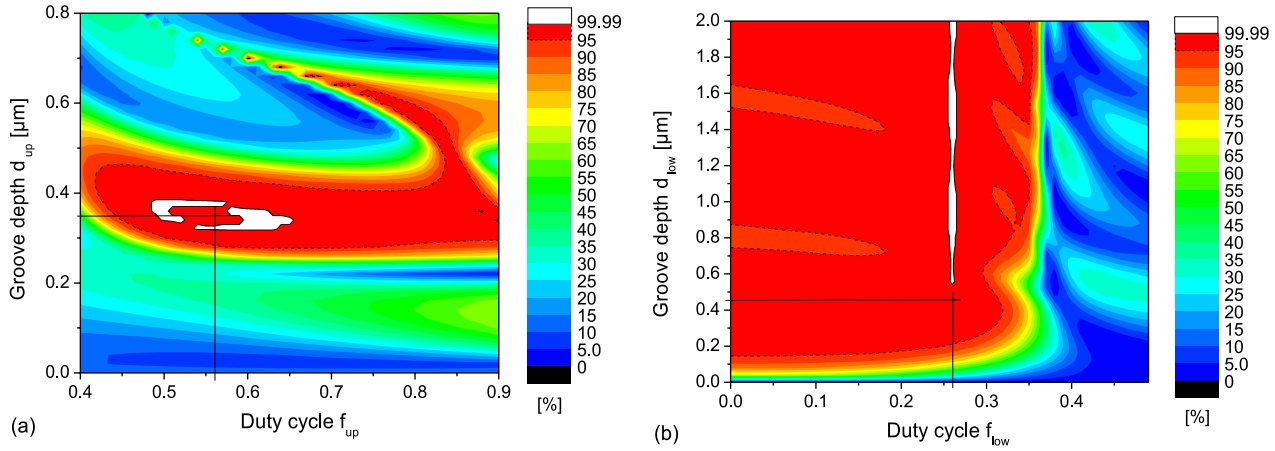


Figure 3. (a) TM-reflectivity over duty cycle $f_{\mathrm{up}}$ and groove depth $d_{\mathrm{up}}$ for fixed parameters $f_{\mathrm{low}} = 0.25$ and $d_{\mathrm{low}} = 2\ \mu$m; (b) TM-reflectivity over duty cycle $f_{\mathrm{low}}$ and groove depth $d_{\mathrm{low}}$ for fixed parameters $f_{\mathrm{up}} = 0.56$ and $d_{\mathrm{up}} = 350\,$nm.

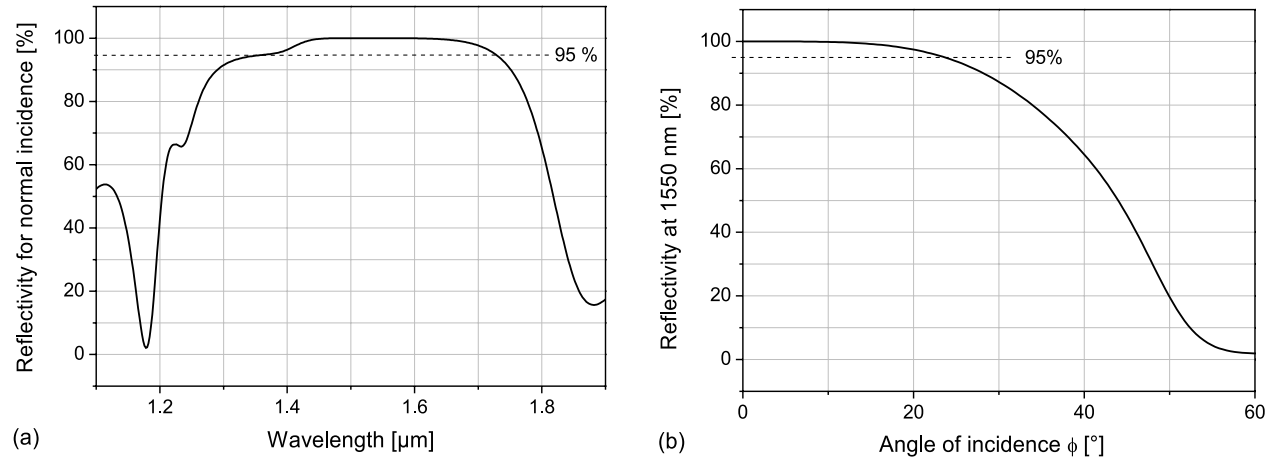


Figure 4. (a) Spectral and (b) angular behavior of the TM-reflectivity for the parameters given in Eqs. (4).

The simulated angular and spectral properties of the device are shown in Fig. 4(a) and (b) revealing a 95 % reflectivity for a broad wavelength range of 1550 nm ± 175 nm and an angle of incidence of $\phi = 0^\circ \pm 23^\circ$. The reflectivity even exceeds a value of 99.99 % for $1.48\,\mu\mathrm{m} < \lambda < 1.58\,\mu\mathrm{m}$ and $\phi = 0^\circ \pm 4.5^\circ$, respectively. These tolerances are much larger than what is known from conventional resonant waveguide gratings,[15–17] making the monolithic device an appropriate approach for the realization of efficient mirrors.

### 3.2.2 TE-Polarization

In case of TE-polarized light, we chose a grating period of $p = 800\,$nm. According to the considerations of the TM-case, both parameters of the HDC grating $f_{\mathrm{up}}$ and $d_{\mathrm{up}}$ were varied in the ranges from $0.7 < f_{\mathrm{up}} < 1$ and $270\,\mathrm{nm} < d_{\mathrm{up}} < 470\,\mathrm{nm}$ for an initially fixed LDC grating with $f_{\mathrm{low}} = 0.4$, $d_{\mathrm{low}} = 2\ \mu$m. The calculated

reflectivity is shown in Fig. 5(a). In contrast to Fig. 3(a) no equivalent design point can be found which exhibits convenient fabrication tolerances. However, this plot reveals a remarkable modification of the proposed monolithic mirror architecture since high reflectivity can even be found for a duty cycle of the HDC grating of $f_{\mathrm{up}} = 1$. The emerging grating profile, as depicted in Fig. 6, does not possess T-shaped grating rigdes, but results in a buried LDC grating which is completely covered by a homogeneous high-index layer of a certain thickness. This thickness can be extracted from Fig. 5(a), leading to the TE-design point ($f_{\mathrm{up}}$;$d_{\mathrm{up}}$) = (1;334 nm) of the upper grating. Although the tolerance of the top high-index layer thickness is rather low, this configuration offers new benefits for the device handling and opportunities for the fabrication process, see following paragraph for the latter. Since the grating device exhibits a plane interface to air, it is protected against dust and mechanical damage such as scratches. It is, furthermore, easy to clean in case of surface contamination.

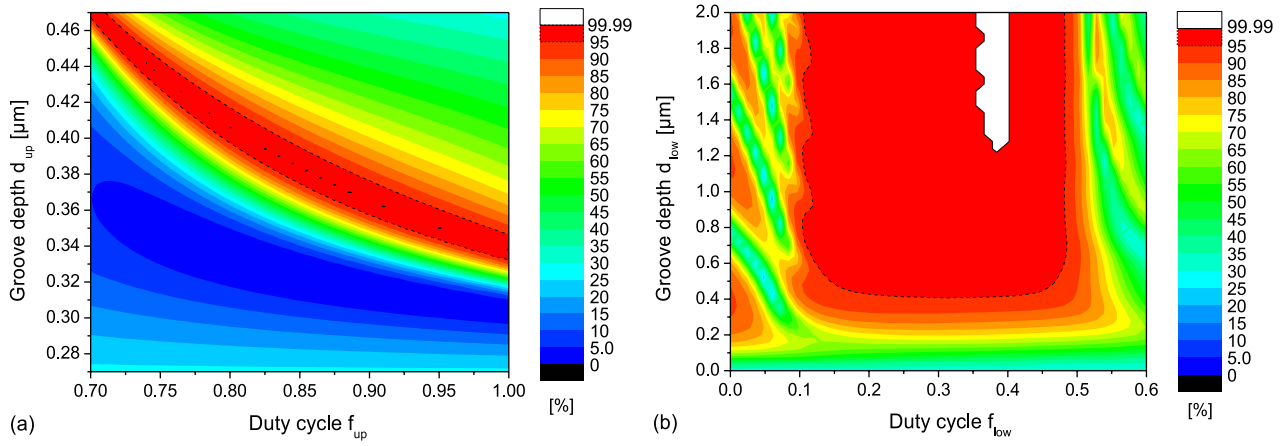


Figure 5. (a) TE-reflectivity over duty cycle $f_{\mathrm{up}}$ and groove depth $d_{\mathrm{up}}$ for fixed parameters $f_{\mathrm{low}} = 0.4$ and $d_{\mathrm{low}} = 2$ $\mu$m; (b) TE-reflectivity over duty cycle $f_{\mathrm{low}}$ and groove depth $d_{\mathrm{low}}$ for fixed parameters $f_{\mathrm{up}} = 1$ and $d_{\mathrm{up}} = 334$ nm.

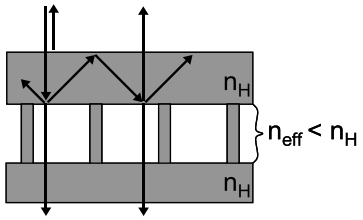


Figure 6. Monolithic mirror architecture with a buried grating, arising from TE-considerations.

In order to examine the fabrication tolerances of the lower grating for the found design point, its parameters were varied as well ranging from $0 < f_{\mathrm{low}} < 0.6$ and $0 < d_{\mathrm{low}} < 2$ $\mu$m, respectively. The reflectivity is plotted in Fig. 5(b), being in general agreement with Fig. 3(b). A wide range of high reflectivity is indicated by the dashed line; values even exceeding 99.99 % are within the white area. In this configuration, the LDC grating plays a double role as the former upper grating is now a homogeneous layer that does not generate any higher diffraction orders or grating modes, respectively. In addition to providing an effective low-index layer which prevents transmission of higher grating modes, the LDC grating simultaneously excites higher orders in reflection, namely within the homogeneous top layer, referring to Ineq. (2) and Fig. 6. Since the excitation of higher orders in reflection is pretty weak, efficient light coupling behavior is highly resonant in agreement with Fig 5(a). The most beneficial parameter values arising from the simulation for TE-polarized light are, at a glance:

$$\begin{array}{rcl} n_{\mathrm{H}} &=& 3.5 \\ \lambda &=& 1550\,\mathrm{nm} \\ \phi &=& 0^\circ \\ p &=& 800\,\mathrm{nm} \end{array} \quad \Longrightarrow \quad \begin{array}{rcl} f_{\mathrm{low}} &=& 0.4 \\ d_{\mathrm{low}} &=& 1300\,\mathrm{nm} \\ f_{\mathrm{up}} &=& 1 \\ d_{\mathrm{up}} &=& 334\,\mathrm{nm}. \end{array} \tag{5}$$

The simulated angular and spectral properties of the buried grating device are shown in Fig. 7(a) and (b), revealing a 95 % reflectivity for a wavelength range of 1550 nm ± 25 nm and an angle of incidence of $\phi = 0° \pm 6°$.

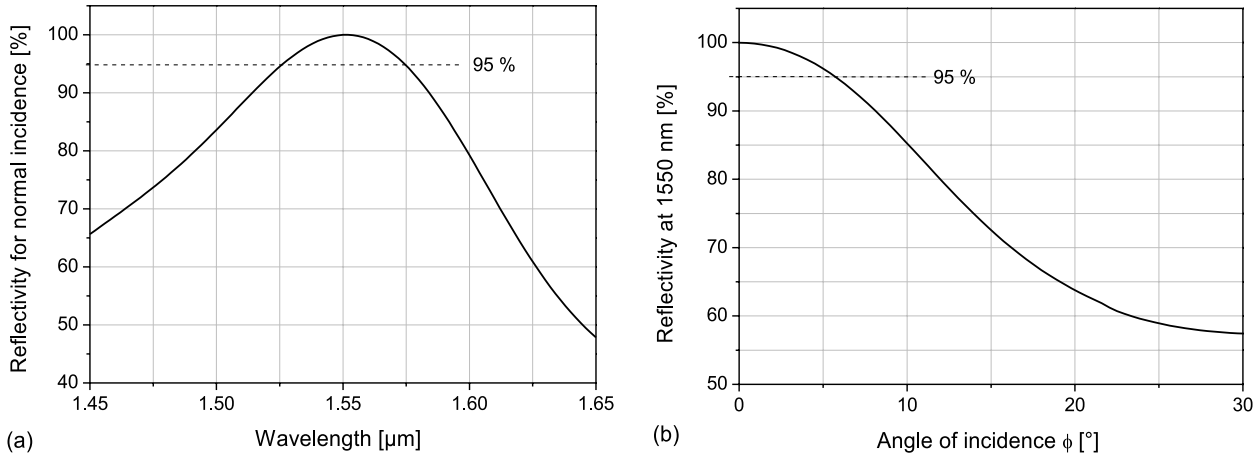


Figure 7. (a) Spectral and (b) angular behavior of the TE-reflectivity for the parameters given in Eqs. (5).

### 3.3 Fabrication Process

The fabrication process is currently in progress and remains a challenging issue. One possible route for T-shaped grating ridges is closely associated with the recently introduced fabrication of microdisks.[25] It is based on a stepwise etching process. As a great benefit for the process, which can be extracted from Fig. 3, the grating profile is not severely limited to a rectangular shape. It may vary arbitrarily within the tolerances, predicting high reflectivity. As mentioned above, the simulated buried grating structure for high TE-reflectivity potentially involves supplemental fabrication techniques. A surface relief grating (LDC grating) which is produced by means of electron beam lithography might be covered by a combined process of silicon coating and subsequent planarization. However, the potential influence of the coated layer on the substrate's mechanical quality factor needs to be precisely investigated. Another approach builds on the well established direct wafer bonding of silicon that allows for covering the surface relief grating by another silicon wafer of certain thickness.[26] Experimental results will be presented in an extended paper.

## 4. CONCLUSION

The proposed novel monolithic mirror architecture offers new routes for many fields of experimental physics. By exciting resonant discrete grating modes within a subwavelength grating and introducing an effective low-index layer, high reflectivity for light incident from air can be achieved in terms of polarization dependency. The effective low-index layer is composed of a grating as well, however, it exhibits a very low duty cycle. Thus, a T-shaped grating profile arises, which allows for a long-term stable mirror device. Since no additional material is needed, conventional resonant waveguide devices can be advanced to prevent mechanical as well as optical loss. Particular design considerations were presented for a silicon surface providing a nearly perfect reflectivity for TM- and TE-polarized light at a 1550 nm wavelength in a large angular and spectral width. The basic idea of this work is part of our patent application.[27] As a matter of course, our approach can also be expanded to other materials and wavelength regions, respectively, by means of parameter scaling. For future work we will address polarization effects more intensively in relation to polarizing beam splitters as well as polarization independent mirror devices.

## ACKNOWLEDGMENTS

This work is supported by the Deutsche Forschungsgemeinschaft within the Sonderforschungsbereich TR7.

## REFERENCES

1. P. F. Cohadon, A. Heidmann, M. Pinard, "Cooling of a Mirror by Radiation Pressure," Phys. Rev. Lett. **83**, 3174 (1999).
2. D. Kleckner, D. Bouwmeester, "Sub-kelvin optical cooling of a micromechanical resonator," Nature **444**, 75 (2006).
3. T. Corbitt, Y. Chen, E. Innerhofer, H. Müller-Ebhardt, D. Ottaway, H. Rehbein, D. Sigg, S. Whitcomb, C. Wipf, N. Mavalvala, "An All-Optical Trap for a Gram-Scale Mirror," Phys. Rev. Lett. **98**, 150802 (2007).
4. S. Mancini, V. Giovannetti, D. Vitali, P. Tombesi, "Entangling Macroscopic Oscillators Exploiting Radiation Pressure," Phys. Rev. Lett. **88**, 120401 (2002)
5. H. Müller-Ebhardt, H. Rehbein, R. Schnabel, K. Danzmann, Y. Chen, "Entanglement of macroscopic test masses and the Standard Quantum Limit in laser interferometry," arXiv:quant-ph/0702258v3 (2007).
6. V. B. Braginsky, F. Y. Khalili, "Quantum nondemolition measurements: the route from toys to tools," Rev. Mod. Phys. **68**, 1 (1996).
7. H. J. Kimble, Y. Levin, A. B. Matsko, K. S. Thorne, S. P. Vyatchanin, "Conversion of conventional gravitational-wave interferometers into quantum nondemolition interferometers by modifying their input and output optics," Phys. Rev D. **65**, 022002 (2001).
8. P. Aufmuth, K. Danzmann, "Gravitational wave detectors," New J. Phys. **7**, 202 (2005).
9. Y. Levin, "Internal thermal noise in the LIGO test masses: A direct approach," Phys. Rev. D **57**, 659 (1998).
10. F. Marquardt, J. P. Chen, A. A. Clerk, S. M. Girvin, "Quantum Theory of Cavity-Assisted Sideband Cooling of Mechanical Motion," Phys. Rev. Lett. **99**, 093902 (2007).
11. G. Rempe, R. J. Thompson, H. J. Kimble, R. Lalezari, "Measurement of ultralow losses in an optical interferometer," Opt. Lett. **17**, 363 (1992).
12. D. F. McGuigan, C. C. Lam, R. Q. Gram, A. W. Hoffman, D. H. Douglass, H. W. Gutche, "Measurements of the Mechanical Q of Single-Crystal Silicon at Low Temperatures," J. Low Temp. Phys. **30**, 621 (1978).
13. G. M. Harry, A. M. Gretarsson, P. R. Saulson, S. E. Kittelberger, S. D. Penn, W. J. Startin, S. Rowan, M. M. Fejer, D. R. M. Crooks, G. Cagnoli, J. Hough, N. Nakagawa, "Thermal noise in interferometric gravitational wave detectors due to dielectric optical coatings," Class. Quantum Grav. **19**, 897 (2002).
14. A. Bunkowski, O. Burmeister, D. Friedrich, K. Danzmann, R. Schnabel, "High reflectivity grating waveguide coatings for 1064 nm," Class. Quantum Grav. **23**, 7297 (2006).
15. G. A. Golubenko, A. S. Svakhin, V. A. Sychugov, A. V. Tishchenko, "Total reflection of light from a corrugated surface of a dielectric waveguide," Sov. J. Quantum Electron. **15**, 886 (1985).
16. R. Magnusson, S. S. Wang, "New principle for optical filters," Appl. Phys. Lett. **61**, 1022 (1992).
17. A. Sharon, D. Rosenblatt, A. A. Friesem, "Resonant grating-waveguide structures for visible and near-infrared radiation," J. Opt. Soc. Am. A **14**, 2985 (1997).
18. C. F. R. Mateus, M. C. Y. Huang, Y. Deng, A. R. Neureuther, C. J. Chang-Hasnain, "Broad-Band Mirror (1.12 - 1.62 m) Using a Subwavelength Grating," IEEE Phot. Techn. Lett. **16**, 518 (2004).
19. J.-S. Ye, Y. Kanamori, F.-R. Hu, K. Hane, "Self-supported subwavelength gratings with a broad band of high reflectance analysed by the rigorous coupled-wave method," J. Mod. Opt. **53**, 1995 (2006).
20. P. Lalanne, D. Lemercier-Lalanne, "On the effective medium theory of subwavelength periodic structures," J. Mod. Opt. **43**, 2063 (1996).
21. L. C. Botten, M. S. Craig, R. C. McPhedran, J. L. Adams, J. R. Andrewartha, "The dielectric lamellar diffraction grating," Opt. Acta **28**, 413 (1981).
22. T. Clausnitzer, T. Kämpfe, E.-B. Kley, A. Tünnermann, U. Peschel, A. V. Tishchenko, O. Parriaux, "An intelligible explanation of highly-efficient diffraction in deep dielectric rectangular transmission gratings," Opt. Express **13**, 10448 (2005).

23. R. Nawrodt, A. Zimmer, T. Koettig, T. Clausnitzer, A. Bunkowski, E.-B. Kley, R. Schnabel, K. Danzmann, W. Vodel, A. Tünnermann, P. Seidel, "Mechanical Q-factor measurements on a test mass with a structured surface," New J. Phys. **9**, 225 (2007).
24. M. G. Moharam, T. K. Gaylord, "Rigorous coupled-wave analysis of planar-grating diffraction," J. Opt. Soc. Am. **71**, 811 (1981).
25. T. J. Kippenberg, J. Kalkman, A. Polman, K. J. Vahala, "Demonstration of an erbium-doped microdisk laser on a silicon chip," Phys. Rev. A **74**, 051802-1 (2006).
26. G. Kräuter, A. Schumacher, U. Gösele, "Low temperature silicon direct bonding for applications in micromechanics: bonding energies for different combinations of oxides," Sensors and Actuators A **70**, 271 (1998).
27. F. Brückner, T. Clausnitzer, E.-B. Kley, "Mikrostrukturierte monolithische dielektrische Oberfläche zur Kontrolle der polarisationsselektiven Reflektivität," German Patent Application 102007047681.9 (2007).